Journal of University of Science and Technology Beijing
Volume 12, Number 3, June 2005, Page 236

Materials

Frequency-dependent dynamic effective properties of porous materials

Peijun Wei[1] *and Zhuping Huang*[2]

1) Applied Science School, University of Sciences and Technology Beijing, Beijing 100083, China
2) Department of Mechanics and Engineering Sciences, Peking University, Beijing 100080, China
(Received 2004-11-23)

Abstract: The frequency-dependent dynamic effective properties (phase velocity, attenuation and elastic modulus) of porous materials are studied numerically. The coherent plane longitudinal and shear wave equations, which are obtained by averaging on the multiple scattering fields, are used to evaluate the frequency-dependent dynamic effective properties of a porous material. It is found that the prediction of the dynamic effective properties includes the size effects of voids which are not included in most prediction of the traditional static effective properties. The prediction of the dynamic effective elastic modulus at a relatively low frequency range is compared with that of the traditional static effective elastic modulus, and the dynamic effective elastic modulus is found to be very close to the Hashin-Shtrikman upper bound.

Key words: dynamic effective properties; porous material; size effects; multiple scattering

[This work was financially supported by the National Natural Science Foundation of China (No.10272003, No.10032010, and No.10372004) and the Talent Foundation of the University of Sciences and Technology Beijing.]

1 Introduction

The determination of the effective propagation constants of waves propagating through composite materials was a subject which attracted a considerable attention in the past several decades [1-9]. A scalar wave propagating through an inhomogeneous medium with distributed particles is first studied by Foldy based on the multiple scattering theory [1]. In this theory a set of equations in hierarchy, each containing more statistical distribution information than those preceding, is involved. In order to truncate these equations to obtain an approximate solution, a self-consistent approximation was given. Later, in order to consider better the distribution correlation between two particles the well-known "quasi-crystalline approximation" was proposed by Lax [2]. Varadan *et al.* [4] and Datta [5] further extended the multiple scattering theory of a scalar wave to elastic waves. Henceforth, the effective propagation constants of the elastic longitudinal and shear waves through a composite medium are extensively studied with consideration of the influence of interface, interphase and the viscosity of material [6-9].

The closed-cell porous material can be considered as a special composite material in which the second phase is the isolated voids. The propagation of waves through such a composite material was studied by Sayers [10-11], Kligman [12], Gubernatis [13], and Varadan [14]. The "superviscous" propagation, void resonance and their corresponding frequency range were investigated. These distinctive characteristics of wave propagation in the porous material are very important in the non-destructive characterization of porous materials. No doubt, the porosity of a porous material is the most important constant and can affect the dynamic effective properties significantly. Varadan [14] studied the effects of porosity on the dynamic effective moduli of rubberlike materials with random distributed voids. It was found that the so-called "superviscous" propagation occurs over a bandwidth controlled by porosity. Sayers [10-11] pointed out that the prediction of the effective properties by Waterman's equation gives a physically impossible result for high porosity and therefore presents a new self-consistent approach which has a reasonable behavior at high porosity. However, the study on the size effects of voids at a fixed porosity is rare in the open literatures. It is the purpose in the present paper to study the size effects of voids on the dynamic effective properties at a fixed porosity. In addition, the dynamic effective moduli obtained from the present scattering theo-

Corresponding author: Peijun Wei, **E-mail:** weipj@126.com

ry at a relatively low frequency range will be compared with the static effective moduli to show the reasonable trend as frequency tends to zero. The outline of the paper is as follows: in section 2, a void scattering problem is studied and the forward scattering amplitudes are formulated. In section 3, the dispersion equations of coherent waves, in which the effective wavenumber is evaluated by using the forward scattering amplitudes of a single scatterer, are discussed. In section 4, the size effects of distributed voids on the dynamic effective properties are studied numerically. The dynamic effective moduli obtained from the present scattering theory at a relatively low frequency range are also compared with the static effective moduli. Finally, some conclusions are given in section 5.

2 Scattered waves by a spherical void

Consider a spherical void of radius a embedded in an elastic matrix. The lam'e constants and the mass density of the matrix material are denoted by $(\lambda_0, \mu_0, \rho_0)$. The geometry is depicted in **figure 1**, where (x, y, z) is the right-handed rectangular Cartesian coordinate system with the origin at the center of the void and (r, θ, ϕ) is the corresponding spherical polar coordinate. Two incident plane longitudinal and shear waves, namely P and S waves, of circular frequency ω are assumed to propagate through the matrix material along the Z-axis and can be expressed by

$$\boldsymbol{u}^{\mathrm{i}} = \boldsymbol{a}\mathrm{e}^{\mathrm{i}(k_{\mathrm{p}0}z-\omega t)} + \boldsymbol{b}\mathrm{e}^{\mathrm{i}(k_{\mathrm{s}0}z-\omega t)} \tag{1}$$

where $\boldsymbol{a} = a\boldsymbol{e}_z$ and $\boldsymbol{b} = b\boldsymbol{e}_x$ are the polarization vectors of incident P and S waves, respectively; $\boldsymbol{e}_z$ and $\boldsymbol{e}_x$ are the unit coordinate vectors; $k_{\mathrm{p}0}$ and $k_{\mathrm{s}0}$ are the wavenumbers of incident P and S waves. When the incident waves impinge the void, the scattered waves are induced.

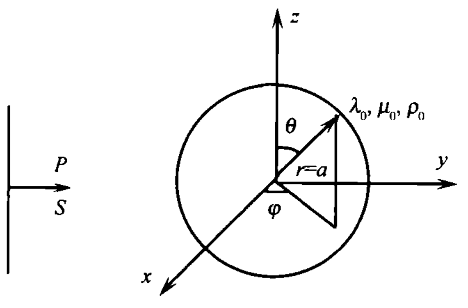

Figure 1 Scattered waves by a spherical void embedded in an elastic matrix.

In order to evaluate the scattered waves in the elastic matrix, we make use of the equation of wave motion in an isotropically elastic solid,

$$k_{\mathrm{p}0}^{-2}\nabla(\nabla\cdot\boldsymbol{u}) - k_{\mathrm{s}0}^{-2}\nabla\times\nabla\times\boldsymbol{u} + \boldsymbol{u} = 0 \tag{2}$$

where ∇ is the gradient operator. $k_{\mathrm{p}0} = \omega/\sqrt{(\lambda_0+2\mu_0)/\rho_0}$ and $k_{\mathrm{s}0} = \omega/\sqrt{\mu_0/\rho_0}$ are the wavenumbers of the longitudinal and the shear waves, respectively. $\boldsymbol{u}(x, y, z, t)$ is the time harmonic displacement vector. For convenience, the time harmonic factor $\mathrm{e}^{-\mathrm{i}\omega t}$ is omitted in the following discussion but understood. It is known that the general form of the solution of equation (2) can be expressed as,

$$\boldsymbol{u} = \nabla\Phi + \nabla\times(\Psi r)\boldsymbol{e}_r + \nabla\times\nabla\times(\Pi r)\boldsymbol{e}_r \tag{3}$$

where the scalar potentials Φ, Ψ and Π satisfy singly the scalar Helmholtz equations,

$$(\nabla^2 + k^2)(\Phi, \Psi, \Pi) = 0 \tag{4}$$

(where ∇^2 is the Laplace operator) and can be expressed in the series form,

$$(\Phi, \Psi, \Pi) = \sum_{n=0}^{\infty}\sum_{m=0}^{\pm n} C_{nm} Z_n^q(kr) P_n^m(\cos\theta)\mathrm{e}^{\mathrm{i}m\phi}$$

$$(q = 1 \text{ or } 3) \tag{5}$$

where C_{nm} is the expansion coefficient, $P_n^m(\cos\theta)$ is the associated Legendre function and the symbol $Z_n^q(kr)$ stands for the spherical Bessel function $j_n(kr)$ for $q=1$ and the spherical Hankel function $h_n^{(1)}(kr)$ for $q=3$. In order to meet the radial conditions at infinity, the potentials of the scattered waves can be expressed as,

$$\begin{cases} \Phi^{\mathrm{s}} = \sum_{n=0}^{\infty}\sum_{m=0}^{\pm n} A_{mn}^{\mathrm{s}} h_n^{(1)}(k_{\mathrm{p}0}r) P_n^m(\cos\theta)\mathrm{e}^{\mathrm{i}m\phi} \\ \Psi^{\mathrm{s}} = \sum_{n=0}^{\infty}\sum_{m=0}^{\pm n} B_{mn}^{\mathrm{s}} h_n^{(1)}(k_{\mathrm{s}0}r) P_n^m(\cos\theta)\mathrm{e}^{\mathrm{i}m\phi} \\ \Pi^{\mathrm{s}} = \sum_{n=0}^{\infty}\sum_{m=0}^{\pm n} C_{mn}^{\mathrm{s}} h_n^{(1)}(k_{\mathrm{s}0}r) P_n^m(\cos\theta)\mathrm{e}^{\mathrm{i}m\phi} \end{cases} \tag{6}$$

where A_{mn}^{s}, B_{mn}^{s} and C_{mn}^{s} are the expansion coefficients to be determined. These expansion coefficients can be determined by the use of the boundary conditions. In the present problem, the boundary conditions is traction-free on the void surface, namely

$$[(\boldsymbol{\sigma}^{\mathrm{i}} + \boldsymbol{\sigma}^{\mathrm{s}})\boldsymbol{n}]\,|_{r=a} = 0 \tag{7}$$

where $\boldsymbol{\sigma} = \lambda(\nabla\cdot\boldsymbol{u})\boldsymbol{\delta} + \mu(\nabla\boldsymbol{u} + \boldsymbol{u}\nabla)$ is the stress tensor. $\boldsymbol{\sigma}^{\mathrm{i}}$ and $\boldsymbol{\sigma}^{\mathrm{s}}$ are corresponding to the incident waves and the scattered waves, respectively. $\boldsymbol{n}$ is the normal vector of the void surface. Further, from the asymptotic expression of radial functions,

$$h_n^{(1)}(kr) \sim \frac{1}{kr}\mathrm{e}^{\mathrm{i}[kr-\frac{1}{2}(n+1)\pi]} + o\left(\frac{1}{r}\right) \qquad (r\to\infty) \tag{8}$$

the displacement of the scattered waves in far-field can be expressed asymptotically,

$$\begin{cases} u_r^s \sim \dfrac{1}{r}\mathrm{e}^{\mathrm{i}k_{p0}r}\sum_{n=0}^{\infty}\sum_{m=0}^{\pm n}\mathrm{i}A_{mn}^s\mathrm{e}^{-\mathrm{i}\frac{1}{2}(n+1)\pi}P_n^m(\cos\theta)\mathrm{e}^{\mathrm{i}m\phi}+o\left(\dfrac{1}{r}\right)=\dfrac{F_r(\theta,\phi)}{r}\mathrm{e}^{\mathrm{i}k_{p0}r}+o\left(\dfrac{1}{r}\right) \\ u_\theta^s \sim \dfrac{1}{r}\mathrm{e}^{\mathrm{i}k_{s0}r}\sum_{n=0}^{\infty}\sum_{m=0}^{\pm n}\mathrm{i}\mathrm{e}^{-\mathrm{i}\frac{1}{2}(n+1)\pi}[B_{mn}^s\dfrac{m}{k_{s0}\sin\theta}P_n^m(\cos\theta)+C_{mn}^s\dfrac{\mathrm{d}}{\mathrm{d}\theta}P_n^m(\cos\theta)]\mathrm{e}^{\mathrm{i}m\phi}+o\left(\dfrac{1}{r}\right)=\dfrac{F_\theta(\theta,\phi)}{r}\mathrm{e}^{\mathrm{i}k_{s0}r}+o\left(\dfrac{1}{r}\right) \\ u_\phi^s \sim -\dfrac{1}{r}\mathrm{e}^{\mathrm{i}k_{s0}r}\sum_{n=0}^{\infty}\sum_{m=0}^{\pm n}[\dfrac{B_{mn}^s}{k_{s0}}\dfrac{\mathrm{d}}{\mathrm{d}\theta}P_n^m(\cos\theta)+\dfrac{m}{\sin\theta}C_{mn}^sP_n^m(\cos\theta)]\mathrm{e}^{-\mathrm{i}\frac{1}{2}(n+1)\pi}\mathrm{e}^{\mathrm{i}m\phi}+o\left(\dfrac{1}{r}\right)=\dfrac{F_\phi(\theta,\phi)}{r}\mathrm{e}^{\mathrm{i}k_{s0}r}+o\left(\dfrac{1}{r}\right) \end{cases} \tag{9}$$

or in a more compact form,

$$\boldsymbol{u}^s \sim \frac{\boldsymbol{F}_p(\theta,\phi)}{r}\mathrm{e}^{\mathrm{i}k_{p0}r}+\frac{\boldsymbol{F}_s(\theta,\phi)}{r}\mathrm{e}^{\mathrm{i}k_{s0}r}+o\left(\frac{1}{r}\right) \tag{10}$$

where $\boldsymbol{F}_p(\theta,\phi)$ and $\boldsymbol{F}_s(\theta,\phi)$ are called the far-field scattered amplitude vectors corresponding to the scattered longitudinal and shear waves.

3 Dynamic effective properties of porous material

We now consider a composite material with N inclusions randomly distributed in the matrix. If their positions of these inclusions, denoted by the random variables ($\boldsymbol{r}_1,\boldsymbol{r}_2,\cdots,\boldsymbol{r}_N$), are given, we shall say that we have a particular configuration of these scatterers. The joint probabilities distribution, denoted by $p(\boldsymbol{r}_1,\boldsymbol{r}_2,\cdots,\boldsymbol{r}_N)$, represents the probability of finding these scatterers in the above configuration. In the composite material with randomly distributed inclusions, the total field at any point $\boldsymbol{r}$ outside all scatterers can be given in the multiple scattering form,

$$\boldsymbol{u}(\boldsymbol{r};\boldsymbol{r}_1,\boldsymbol{r}_2,\cdots,\boldsymbol{r}_N)=\boldsymbol{u}^{\mathrm{i}}(\boldsymbol{r})+\sum_{k=1}^{N}\boldsymbol{T}^s(\boldsymbol{r}_k)\boldsymbol{u}^{\mathrm{i}}(\boldsymbol{r})+\sum_{m=1}^{N}\boldsymbol{T}^s(\boldsymbol{r}_m)\sum_{k=1,k\neq m}^{N}\boldsymbol{T}^s(\boldsymbol{r}_k)\boldsymbol{u}^{\mathrm{i}}(\boldsymbol{r})+\cdots \tag{11}$$

where the single summation denotes the primary scattered terms, the double summation denotes the secondary terms and so on. The primary scattering is due to the incident waves alone, and the second scattering represents the rescattering of the primary scattered waves, etc. The coherent wave field is defined as the configurational average of the total wave field

$$\langle \boldsymbol{u}(\boldsymbol{r}\,|\,\boldsymbol{r}_1,\cdots,\boldsymbol{r}_N)\rangle=\int\cdots\int \boldsymbol{u}(\boldsymbol{r}\,|\,\boldsymbol{r}_1,\cdots,\boldsymbol{r}_N)p(\boldsymbol{r}_1,\cdots,\boldsymbol{r}_N)\mathrm{d}V_1\cdots\mathrm{d}V_N \tag{12}$$

where the first coordinate $\boldsymbol{r}$ indicates the field point of evaluation, and the ($\boldsymbol{r}_1,\cdots,\boldsymbol{r}_N$) indicates the dependence of the random function $\boldsymbol{u}$ on the specific configuration chosen. The total wave field can also be regarded as the sum of the coherent wave field (the mean wave field) and the fluctuating wave field. The mean wave field can be considered as the wave field propagating in the homogeneous medium having the effective properties of the composite and the fluctuating wave field can be considered as the wave field due to the spatial randomly variations of material properties from those of the effective medium. This can be expressed as,

$$\boldsymbol{u}(\boldsymbol{r})=\bar{\boldsymbol{u}}(\boldsymbol{r})+\tilde{\boldsymbol{u}}(\boldsymbol{r}) \tag{13}$$

where

$$\bar{\boldsymbol{u}}(\boldsymbol{r})=\boldsymbol{a}^*\mathrm{e}^{\mathrm{i}(k_{p*}z-\omega t)}+\boldsymbol{b}^*\mathrm{e}^{\mathrm{i}(k_{s*}z-\omega t)} \tag{14}$$

$$\tilde{\boldsymbol{u}}(\boldsymbol{r})=\sum_{i=1}^{N}\bar{\boldsymbol{T}}_i^s\bar{\boldsymbol{u}}(\boldsymbol{r}) \tag{15}$$

where k_{p*} and k_{s*} are the wavenumbers and $\boldsymbol{a}^*$ and $\boldsymbol{b}^*$ are the polarization vectors of the mean P and S waves, respectively. $\bar{\boldsymbol{T}}_i^s$ is the scattering operator of i-th fictive inclusion embedded in the effective medium.

In order to simplify the interaction of particles and to obtain an approximate solution of the mean wave fields, Equation (11) is usually truncated by use of the self-consistent effective field approximation. For the elastic waves propagating through an inhomogeneous medium, based on the effective field approximation and the statistical average procedure, we obtain the dispersion relations of the effective longitudinal and shear waves propagating through the composite material [9],

$$\begin{cases} k_{p*}^2=k_{p0}^2+(\lambda_0+2\mu_0)^{-1}n\bar{T}_{ij}^s a_i a_j \\ k_{s*}^2=k_{s0}^2+\mu_0^{-1}n\bar{T}_{ij}^s b_i b_j \end{cases} \tag{16}$$

Consider that the scattering operator $\bar{\boldsymbol{T}}^s$ of a single inclusion bears a simple relation to the far-field scattering amplitude vectors of the waves scattered by the same inclusion [3],

$$\begin{cases} \bar{T}_{ij}^s a_i a_j=\dfrac{4\pi\rho_0\omega^2}{k_{p0}^2}[\boldsymbol{F}_p(\theta,\phi)\cdot\boldsymbol{a}]\big|_{\theta=0} \\ \bar{T}_{ij}^s b_i b_j=\dfrac{4\pi\rho_0\omega^2}{k_{s0}^2}[\boldsymbol{F}_s(\theta,\phi)\cdot\boldsymbol{b}]\big|_{\theta=0} \end{cases} \tag{17}$$

Equation (16) can be rewritten as

$$\begin{cases} k_{p*}^2=k_{p0}^2+4\pi n[\boldsymbol{F}_p(\theta,\phi)\cdot\boldsymbol{a}]\big|_{\theta=0} \\ k_{s*}^2=k_{s0}^2+4\pi n[\boldsymbol{F}_s(\theta,\phi)\cdot\boldsymbol{b}]\big|_{\theta=0} \end{cases} \tag{18}$$

where $n = N/V$ is the number density of inclusions (N is the numbers of inclusions in a composite material with volume V). $F_p(\theta,\phi)$ and $F_s(\theta,\phi)$ are the frequency and azimuth dependent far-field scattering amplitude vectors given in equation (10). $\theta = 0$ denotes the incident direction. $[F_p(\theta,\phi)\cdot a]\big|_{\theta=0}$ and $[F_s(\theta,\phi)\cdot b]\big|_{\theta=0}$ denote the projections of the forward scattering amplitude vector of incident P and S waves in the polarization direction. In the present scattering problem of the spherical void they can be expressed as

$$\begin{cases} [F_p(\theta,\phi)\cdot a]\big|_{\theta=0} = \sum\limits_{n=0}^{\infty}(-\mathrm{i})^n A_{0n}^{s} \\ [F_s(\theta,\phi)\cdot b]\big|_{\theta=0} = \\ \sum\limits_{n=1}^{\infty}\dfrac{(-i)^n}{2}\{n(n+1)C_{1n} - C_{-1n} + \dfrac{n(n+1)}{k_{s0}}B_{1n} + \dfrac{1}{k_{s0}}B_{-1n}\} \end{cases} \tag{19}$$

Because the far-field scattering amplitudes are complex-valued and frequency-dependent, k_{p*} and k_{s*} are thus complex-valued and frequency-dependent. The real part of complex-valued wavenumber is related to the phase velocities and the imaginary part is related to the attenuation.

$$\begin{cases} k_{p*}(\omega) = k_{p*}^{r}(\omega) + \mathrm{i}k_{p*}^{i}(\omega) = \omega/c_p^* + \mathrm{i}\alpha_p^* \\ k_{s*}(\omega) = k_{s*}^{r}(\omega) + \mathrm{i}k_{s*}^{i}(\omega) = \omega/c_s^* + \mathrm{i}\alpha_s^* \end{cases} \tag{20}$$

where c_p^*, c_s^*, α_p^*, and α_s^* are the phase velocities and the attenuation factors of the effective P and S waves, respectively. The complex-valued propagation constant means an attenuated wave. In other word, the coherent plane waves propagating through an elastic porous medium will be attenuated due to the multiple scattering effects among voids. We know that the general plane waves propagating through a dissipative medium are of the complex-valued wavenumbers. However, the complex-valued wavenumbers result from the energy absorption in the dissipative medium but the energy diffusion in the elastic porous medium. The complex-valued and frequency-dependent dynamic effective elastic constants of the porous medium can be obtained from the effective wavenumbers by

$$\begin{cases} \mu_*(\omega) = \mu_*^r(\omega) + \mathrm{i}\mu_*^i(\omega) = \mu_0\dfrac{\rho_*}{\rho_0}\left(\dfrac{k_{s0}}{k_{s*}}\right)^2 \\ \lambda_*(\omega) = \lambda_*^r(\omega) + \mathrm{i}\lambda_*^i(\omega) = \\ \quad (\lambda_0 + 2\mu_0)\dfrac{\rho_*}{\rho_0}\left(\dfrac{k_{p0}}{k_{p*}}\right)^2 - 2\mu_0\dfrac{\rho_*}{\rho_0}\left(\dfrac{k_{s0}}{k_{s*}}\right)^2 \end{cases} \tag{21}$$

where the effective mass density of the porous medium, ρ_*, can be obtained straightforward from the volume average, namely,

$$\rho_* = (1-c)\rho_0 \tag{22}$$

where c is the porosity of the porous material.

4 Numerical results and discussion

The dynamic effective properties of a porous material modeled by randomly positioned spherical voids in the silicon nitride will be studied numerically. The radii of the distributed spherical voids are assumed to be identical. The elastic moduli and the mass density of the silicon nitride are $\lambda_0 = 1.586$ GPa, $\mu_0 = 1.251$ GPa, $\rho_0 = 3200$ kg/m^3 (from reference [13]).

The predicted effective phase velocities and attenuations as functions of the non-dimensional wavenumber k_0a for the prescribed porosity $c = 0.1$ are shown in **figure 2** (a) and (b), respectively. The effective phase velocity v_* is normalized by $(v_* - v_0)/(cv_0)$ (v_0 is the phase velocity of the host medium) in order to compare expediently the present numerical results with that obtained by others. The validity of our FORTRAN code evaluating the effective velocity and attenuation can be verified by the agreement between the present results and those ob-

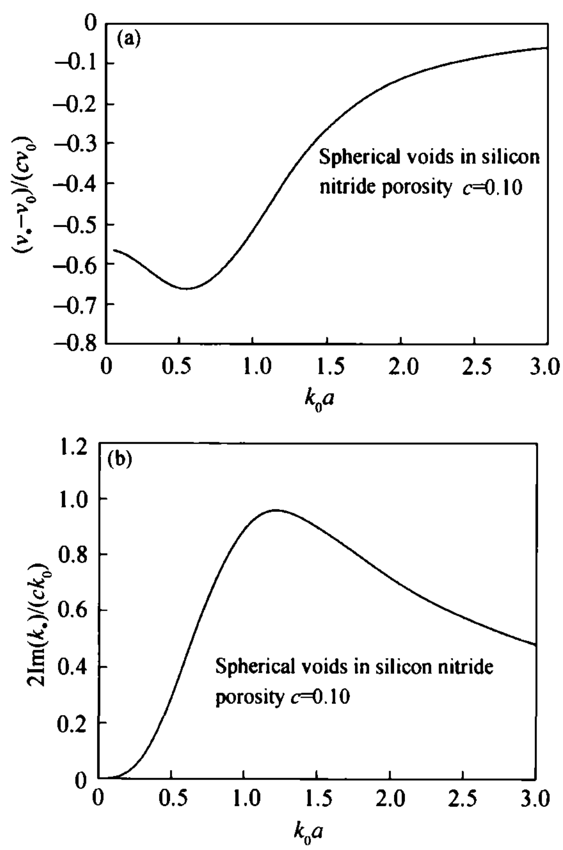

Figure 2 Effective phase velocity and attenuation of porous material with identical radii of voids (porosity c=0.10): (a) effective phase velocity; (b) effective attenuation.

tained by Gubernatis & Domany [13]. The numerical results show that the effective phase velocities are always smaller than the phase velocities of the host material. Moreover, the effective phase velocities decrease from the static prediction with the increase of non-dimension wavenumber $k_0 a$ at the initial stage and start to increase after about $k_0 a \approx 0.5$ and then gradually tend to the velocities of the host material. The normalized effective attenuation, *i.e.* $2\mathrm{Im}(k_*)/(ck_0)$, increases from zero and reaches a peak at about $k_0 a \approx 1.2$ and then decrease gradually with the increase of non-dimension wavenumber $k_0 a$. It is noticed that the observations are the same for both longitudinal and shear waves for that our numerical results are scaled by k_0 which denotes k_{p0} and k_{s0} for P and S waves, respectively.

The static effective moduli of porous materials have been investigated extensively. Up to now, a number of methods can be used to obtain the prediction of static effective moduli, for example, the differential scheme, the Mori-Tanaka method, the self-consistent and generalized self-consistent methods. Moreover, Voigt bound, Reuss bound and the more narrow Hashin-Shtrikman bounds are also used to predict the range of possible effective constants. Nevertheless, all these methods mentioned above can't reveal the size effects of the voids. It is an advantage of the present method that the dynamic effective moduli obtained from the present scattering theory includes the size effects. The effects of the void radius on the effective phase velocities and attenuations of the porous silicon nitride material (porosity c=0.1) are shown in **figure 3**. It is seen that the effects of the radius of voids are obvious. Generally speaking, for a fixed porosity, the bigger voids make the minimum of phase velocities and the maximum of attenuation shift toward low frequency when compared with the smaller voids. The effects of void radius on the effective moduli of the porous material are shown in **figure 4**. An oscillating behavior in a specific frequency region is observed on the curve of the effective moduli as a function of non-dimension wavenumber $k_{s0}a$. This observation agrees with those observed by Kligman [12] and Varadan [14]. The oscillating behavior of breathing mode is related to the resonances of voids. It is shown that the bigger voids make the resonances region shift toward the low frequency when compared with the smaller voids. In addition, the size effects are obvious at the modest and the high frequency region and decrease gradually to zero when the frequency trends to zero.

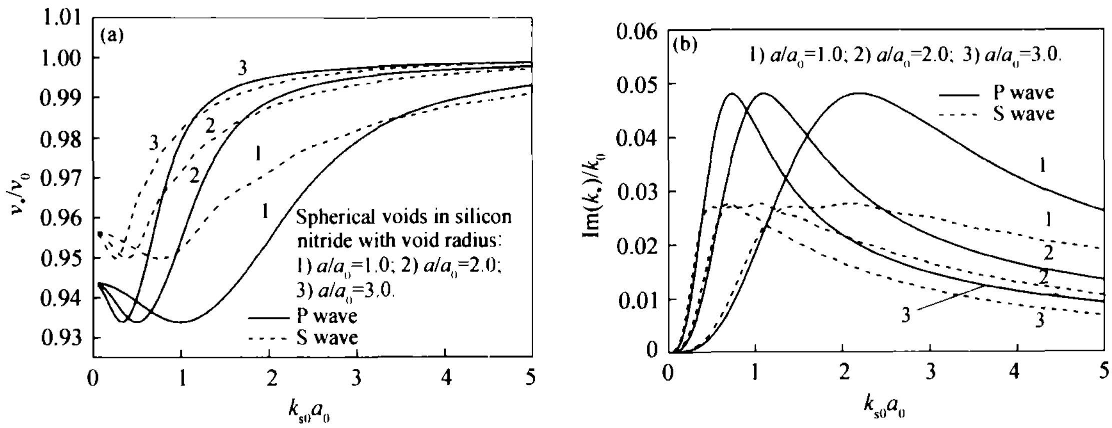

Figure 3 Effects of void radius on the phase velocity and attenuation of the porous material with identical radii of voids (porosity c=0.10): (a) effective phase velocity; (b) effective attenuation.

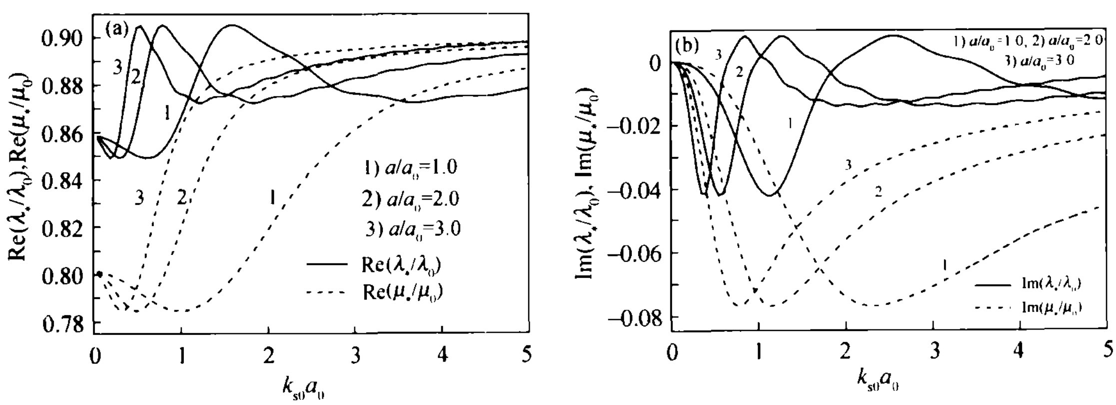

Figure 4 Effects of void radius on the effective complex moduli of the porous material with identical radii of voids (porosity c=0.10): (a) real parts; (b) imaginary parts.

The effects of porosity on the dynamic effective elastic moduli of the porous material with identical void radii are shown in **figure 5**. It is observed that the increase of porosity makes the real parts of the frequency-dependent complex elastic moduli decreasing, whereas the imaginary parts of the frequency-dependent complex elastic moduli increasing in amplitudes. This means that the effective elastic moduli of the porous material decrease and the effective attenuations of the porous material increase. Because the dynamic effective moduli are frequency-dependent, it is expected that the dynamic effective moduli should tend to the static effective moduli as the frequency tends to zero. In **figure 6**, the dynamic effective moduli predicted at a relatively low frequency range are shown together with the static effective moduli predicted by the self-consistent method and their corresponding Voigt bound and Hashin-Shtrikman upper bound (the Reuss bound and the Hashin-Shtrikman down bound are zero for a porous material). It is observed that the effective dynamic moduli tend to the Hashin-Shtrikman upper bound as the frequency tends to zero. Recognizing that the Hashin-Shtrikman upper bound is coincident with the Mori-Tanaka prediction for a porous material, we can also say that the effective dynamic moduli tend to Mori-Tanaka prediction as frequency tends to zero. This can be explained by that the static moduli prediction by Mori-Tanaka method and the dynamic moduli prediction by the present scattering theory are both based on the effective field approach to simplify the interaction among the distributed voids.

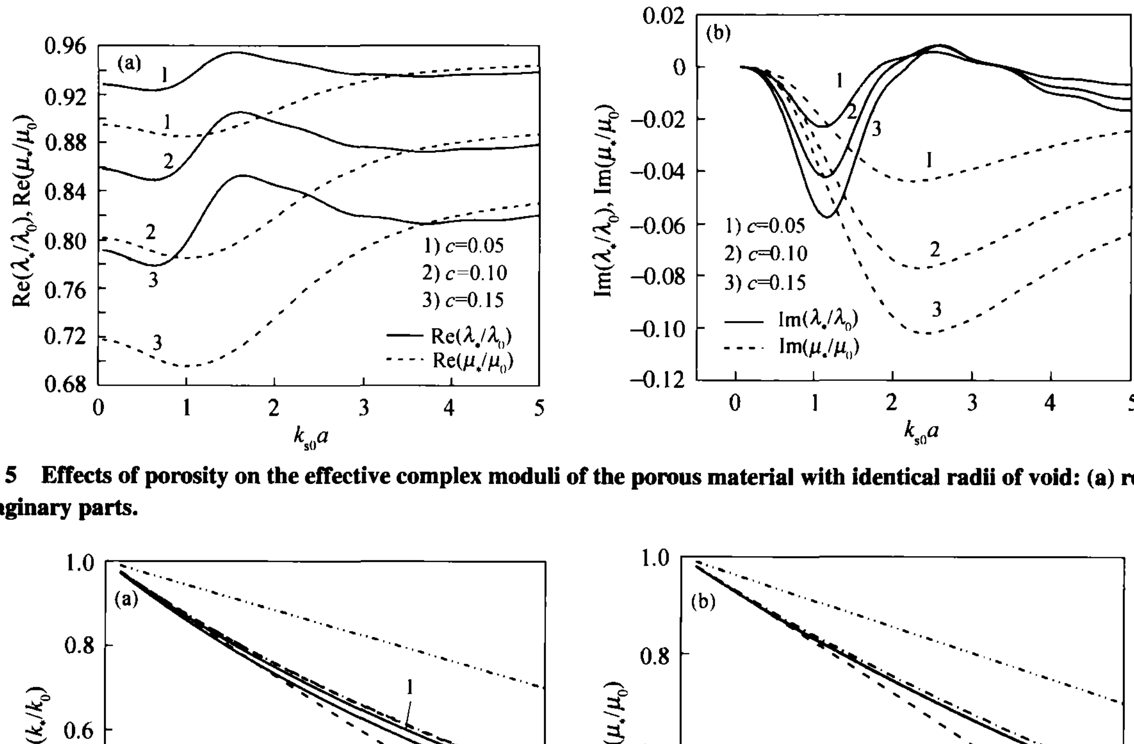

Figure 5 Effects of porosity on the effective complex moduli of the porous material with identical radii of void: (a) real parts; (b) imaginary parts.

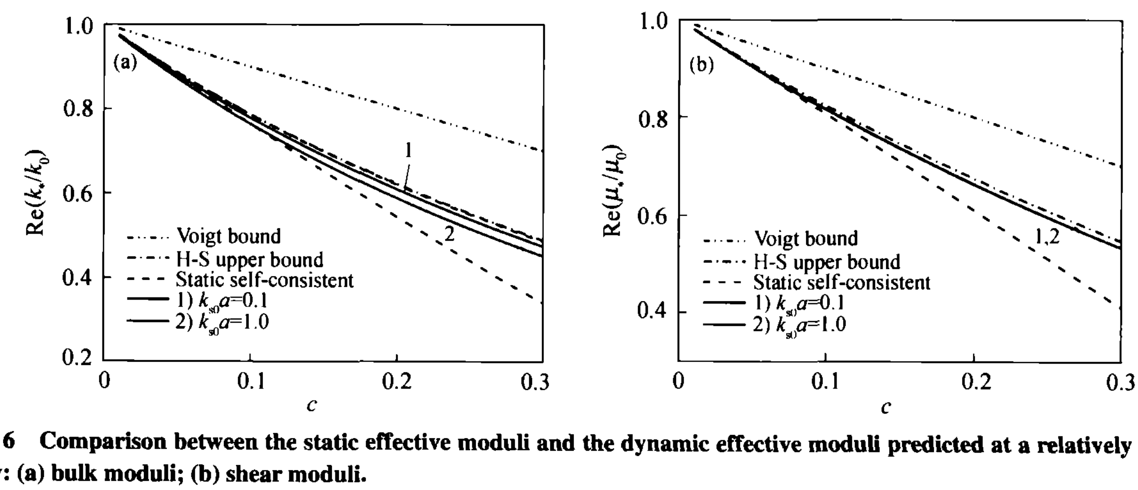

Figure 6 Comparison between the static effective moduli and the dynamic effective moduli predicted at a relatively low frequency: (a) bulk moduli; (b) shear moduli.

5 Conclusions

The dynamic effective moduli predicted by the present scattering theory include the size effects of distributed voids in a porous material. The numerical results show that the size effects are pronounced at a relatively modest and a high frequency range but decrease gradually with the decrease of the frequency. Generally speaking, for a fixed porosity, the bigger voids make the resonances region shift toward the low frequency when compared with the smaller voids. Consequently, the minimum of phase velocities and the maximum of attenuation of the porous material shift also toward low frequency when the radii of voids increase. In addition, due to the dynamic effective moduli are frequency-dependent, it is expected that the dynamic effective moduli should tend to the static effective moduli as the frequency tends to zero. The numerical results show that the dynamic effective moduli predicted by the present scattering theory tend to the static effective moduli predicted by Mori-Tanaka method. The explanation for this comes down to the effective field approach which is used to simplify the interaction among the distributed voids not only in Mori-Tanaka method for the prediction of static effective moduli but also in the present scattering theory for the prediction of dynamic effective moduli.

References

[1] L.O. Foldy, The multiple scattering of waves, *Phys. Rev.*, 67(1945), p.107.

[2] M. Lax, Multiple scattering of waves, *Rev. Mod. Phys.*, 23(1951), p.287.

[3] A.J. Devaney, Multiple scattering theory for discrete elastic random media, *J. Math. Phys.*, 21(1980), p.2603.

[4] V.K. Varadan, Y. Ma, and V.V. Varadan, A multiple scattering theory for elastic waves propagation in discrete random medium, *J. Acoust. Soc. Am.*, 77(1985), p.375.

[5] S.K. Datta, H.M. Ledbetter, and Y. Shindo, Phase velocity and attenuation of plane elastic waves in a particle-reinforced composite medium, *Wave Motion*, 10(1988), p.171.

[6] Y. Shindo, H. Nozaki, and S.K. Datta, Effect of interface layers on elastic wave propagation in a metal matrix composite reinforced by particles, *ASME, J. Appl. Mech.*, 62(1995), p.178.

[7] S. Biwa, Independent scattering and wave attenuation in viscoelastic composites, *Mech. Mater.*, 33(2001), p.635.

[8] S.K. Kanaun, V.M. Levin, and F.J. Sabina, Propagation of elastic waves in composites with random set of spherical inclusion (effective medium approach), *Wave Motion*, 40(2004), p.69.

[9] P.J. Wei and Z.P. Huang, Dynamic effective properties of the particle-reinforced composites with the viscoelastic interphase, *Int. J. Solids Struct.*, 41 (2004), p.6993.

[10] C.M. Sayers and R.L. Smith, The propagation of ultrasound in porous media, *Ultrasonics*, 20(1981), p.201.

[11] C.M. Sayers, Ultrasonic velocity dispersion in porous materials, *J. Phys. D*, 14(1982), p.413.

[12] R.L. Kligman, W.M. Madigosky, and J.R. Barlow, Effective dynamic properties of composite viscoelastic materials, *J. Acoust. Soc. Am.*, 70(1981), p.1437.

[13] J.E. Gubernatis and E. Domany, Effects of microstructure on the speed and attenuation of elastic waves in porous material, *Wave Motion*, 6(1984), p.579.

[14] V.K. Varadan and V.V. Varadan, Frequency dependent elastic properties of rubberlike materials with a random distributed voids, *J. Acoust. Soc. Am.*, 76(1984), p.296.